

Two dimensional symmetric correlation functions of the \hat{S} operator and two dimensional Fourier transforms: Considering the line coupling for P and R lines of linear molecules

Q. Ma,¹ C. Boulet,² and R. H. Tipping³

¹NASA/Goddard Institute for Space Studies and Department of Applied Physics and Applied Mathematics, Columbia University, 2880 Broadway, New York, New York 10025, USA

²Institut des Sciences Moléculaires d'Orsay (ISMO), CNRS (UMR8214) et Université Paris-Sud Bât 350, Campus d'Orsay F-91405, France

³Department of Physics and Astronomy, University of Alabama, Tuscaloosa, Alabama 35487-0324, USA

(Received 8 January 2014; accepted 20 February 2014; published online 12 March 2014)

The refinement of the Robert-Bonamy (RB) formalism by considering the line coupling for isotropic Raman Q lines of linear molecules developed in our previous study [Q. Ma, C. Boulet, and R. H. Tipping, *J. Chem. Phys.* **139**, 034305 (2013)] has been extended to infrared P and R lines. In these calculations, the main task is to derive diagonal and off-diagonal matrix elements of the Liouville operator $iS_1 - S_2$ introduced in the formalism. When one considers the line coupling for isotropic Raman Q lines where their initial and final rotational quantum numbers are identical, the derivations of off-diagonal elements do not require extra correlation functions of the \hat{S} operator and their Fourier transforms except for those used in deriving diagonal elements. In contrast, the derivations for infrared P and R lines become more difficult because they require a lot of new correlation functions and their Fourier transforms. By introducing two dimensional correlation functions labeled by two tensor ranks and making variable changes to become even functions, the derivations only require the latter's two dimensional Fourier transforms evaluated at two modulation frequencies characterizing the averaged energy gap and the frequency detuning between the two coupled transitions. With the coordinate representation, it is easy to accurately derive these two dimensional correlation functions. Meanwhile, by using the sampling theory one is able to effectively evaluate their two dimensional Fourier transforms. Thus, the obstacles in considering the line coupling for P and R lines have been overcome. Numerical calculations have been carried out for the half-widths of both the isotropic Raman Q lines and the infrared P and R lines of C_2H_2 broadened by N_2 . In comparison with values derived from the RB formalism, new calculated values are significantly reduced and become closer to measurements. © 2014 AIP Publishing LLC. [<http://dx.doi.org/10.1063/1.4867417>]

I. INTRODUCTION

Knowledge of molecular spectroscopy is essential for atmospheric sensing, combustion diagnostic, and other scientific and engineering applications. Among all the spectroscopic parameters of transitions, to accurately determine the pressure broadened half-width and the induced shift is the most difficult problem and still remains as a big challenge for experimentalists and theorists. Because the ambient atmospheric species, temperatures, and pressures are not always amenable to laboratory measurements, or because of the large number of transitions possible, one often has to rely on theoretical calculations based on different line shape theories.¹⁻⁵ Among them, the formalism developed by Robert and Bonamy in 1979⁵ is one of the most widely used methods, especially for complicated molecules. The main features of this well known Robert-Bonamy (RB) formalism consist of applying the linked cluster theorem⁶ to evaluate the Liouville scattering \hat{S} operator and introducing an atom-atom model to represent short range interactions.

Mainly due to its importance in practice, a lot of efforts have been made for years in order to improve the RB

formalism.⁷⁻¹⁰ Descriptions of these refinements and modifications have been presented in our previous work,¹¹ they are not repeated here again. Despite all efforts to improve the RB formalism such that with somehow adjustments of potential parameters, the current RB formalism can yield reasonably good agreements with measurements, a series of recent papers^{12,13} have demonstrated that for simpler systems where results of the close coupling calculations⁴ with more sophisticated potentials are available, the RB formalism significantly overestimates the half-widths. Because there is no room to make potential adjustments, the large differences clearly mean the RB formalism itself contains severe weaknesses.

Recently, we have found that when Robert and Bonamy applied the linked cluster theorem to remove the cutoff appearing in Anderson's theory,^{1,2} they have assumed matrix elements of an exponential function of the Liouville operator $iS_1 - S_2$ can be replaced by values of an ordinary exponential function whose arguments are the matrix elements of this operator.¹¹ In other words, they have assumed a behavior of an exponential of the operator looks like an ordinary function. With this replacement, effects from the non-diagonality

nature of this operator are ignored. The validity criterion of this approximation is that in comparison with its diagonal matrix elements, the off-diagonal matrix elements of $iS_1 - S_2$ are negligible. Usually, this simplification is referred to the isolated line approximation, the same name of the approximation with which one ignores the off-diagonal matrix elements of the relaxation operator W in calculating the spectral density $F(\omega)$.

In our previous work,¹¹ we have scrutinized these two simplifying practices in developing the RB formalism and have pointed out intrinsic differences between them. Here, we briefly outline the differences. These two practices deal with different subjects: the non-diagonality (within the linespace) of the operator $\exp(iS_1 - S_2)$ or of the relaxation operator W . Since they cause different consequences, we have proposed in Ref. 11 to name them differently. The line coupling results from off-diagonal matrix elements of $\exp(iS_1 - S_2)$, whereas the line mixing results from off-diagonal elements of the relaxation matrix W . To neglect the line coupling or to neglect the line mixing has a completely different criterion, and the former is more stringent than the latter. A failure to distinguish their different criteria by applying the less stringent one in both the practices could cause large errors. In many cases where the line mixing becomes negligible, effects on calculated half-widths and shifts from the line coupling still remain important and they have been completely ignored.

In our previous work, we have developed a refined RB formalism applicable for isotropic Raman Q lines of linear molecules with which one is able to consider effects on calculated half-widths from the line coupling.¹¹ In developing this formalism, a manipulating technique plays a crucial role to simplify the expression for the off-diagonal matrix elements of $S_{2,\text{middle}}$ such that there are no new correlation functions and their Fourier transforms required here except for those used in deriving the diagonal matrix elements of $S_{2,\text{outer},i}$, $S_{2,\text{outer},f}$, and $S_{2,\text{middle}}$. Because these correlations and Fourier transforms are labeled by two tensor ranks,¹⁰ their numbers are only a few. It is worth mentioning that the manipulation relies on a condition of $\omega_{i'i} = \omega_{f'f}$ which becomes possible only for those coupled lines such that the energy differences between their initial states and between their final states are identical (i.e., $E_{i'} - E_i = E_{f'} - E_f$). It is obvious that for isotropic Raman Q lines of linear molecules, this condition is exact within the rigid rotor limit and remains well applicable when the vibration rotation coupling is taken into account. Then, by using this simple expression, we have derived the off-diagonal elements of $S_{2,\text{middle}}$ and subsequently, we have successfully considered effects on calculated half-widths of isotropic Raman Q lines for N_2 broadened by N_2 from the line coupling. The results have clearly demonstrated the importance of the line coupling.¹¹

Despite this success, there is a weakness remaining in this previous study because the simpler expression is only applicable for isotropic Raman Q lines. For infrared P and R lines where $\omega_{i'i} \neq \omega_{f'f}$, one has to use a general expression in which there are a lot of new correlation functions and their complex Fourier transforms introduced. Because these new functions are not only labeled by the two tensor ranks, but also by other parameters, their numbers increase significantly.

Furthermore, in modern half-width calculations where more accurate potential models and the “exact” collisional trajectory model^{7,8} are adopted, all of these functions have to be numerically evaluated. As a result, one faces a challenge in deriving off-diagonal matrix elements of $S_{2,\text{middle}}$ for P and R lines from the general expression. The problem is such serious that unless one finds a way to simplify this general expression, it becomes very difficult to consider the line coupling for infrared P and R lines at all. Fortunately, we have found that by fully exploiting the coordinate representation, one can introduce two dimensional (2D) correlation functions labeled by the same two tensor ranks. With properly changing variables, one can make them as even functions for both their new variables. Besides, the number of these 2D symmetric functions is very limited. Finally, in terms of the latter’s 2D Fourier transforms, one is able to obtain a simpler expression for the off-diagonal elements of $S_{2,\text{middle}}$.

Besides obtaining the simpler expression, one enjoys other benefits by easily discovering some hiding features of the off-diagonal elements. For example, because the 2D correlation functions are even functions, their 2D Fourier transforms become real. Then, it becomes obvious that the off-diagonal matrix elements of $S_{2,\text{middle}}$ are real too. In addition, the averaged energy gap and the frequency detuning between the two coupled lines appear as the two modulation frequencies of these 2D Fourier transforms in the new expression. Based on this feature, one can conclude that it is these two quantities that characterize the coupling strength between the two coupled lines. Armed with this knowledge, to predict whether the coupling between the two coupled lines is important or not becomes easier and more accurate.

Of course, the success in applying the simpler expression relies on how to effectively and accurately evaluate these 2D Fourier transforms in practical calculations. In our previous works, based on the sampling theory we have developed effective tools to derive one dimensional Fourier transforms from one dimensional correlation functions. By combining the techniques with other approaches available in the signal theory,¹⁴ we are able to successfully derive these 2D Fourier transforms. After the latter are available, there are no more obstacles left in considering the line coupling for P and R lines. Numerical calculations of the half-widths for the infrared P and R lines of C_2H_2 broadened by N_2 based a new potential model¹⁵ together with those for the isotropic Raman Q lines have been carried out. The calculated results clearly demonstrate that effects from the line coupling are important in both these cases. In comparison with values derived from the RB formalism, new calculated values are significantly reduced and become closer to measurements.¹⁶

In Sec. II, we show how to introduce the 2D correlation functions and to change them to become even functions. By exploiting the latter’s symmetry properties, a simpler expression for the off-diagonal matrix elements of $S_{2,\text{middle}}$ can be obtained in terms of their 2D Fourier transforms. With this expression, to calculate the off-diagonal matrix elements for P and R lines becomes more tractable in practical calculations. In Sec. III, we apply the new formula to the $C_2H_2-N_2$ system and present calculated half-widths of the infrared R lines. In Sec. IV, we present discussions and conclusions. With

detailed formula derivations and numerical sample demonstrations presented in Secs. II and III, we believe our refinement of the RB formalism makes another progress in the right direction.

II. THEORY

A. Matrices of $S_{2,outer,i}$, $S_{2,outer,f}$, and $S_{2,middle}$ in the coordinate representation

It has been known for years, when one calculates matrices of $S_{2,outer,i}$, $S_{2,outer,f}$, and $S_{2,middle}$ based on potentials containing site-site model components, one could encounter convergence problems.¹⁷ As demonstrated in our previous

work,¹⁰ a solution is to use the coordinate representation by choosing the orientations of the pair of molecules as the basis set in Hilbert space; i.e., $|\delta(\Omega_a - \Omega_{a\alpha})\rangle \otimes |\delta(\Omega_b - \Omega_{b\alpha})\rangle$, where $\Omega_{a\alpha}$ and $\Omega_{b\alpha}$ represent orientations of the absorber and bath molecules specified by α , respectively. In contrast, with the standard representation, the basis set is constructed from $|i_1 m_1\rangle \otimes |i_2 m_2\rangle$, the product of the states of two interacting molecules. The advantage in choosing the coordinate representation results from a fact that with this representation, the potential becomes a diagonal operator and its matrix elements become multi-dimensional integrations whose angular parts can be evaluated analytically.

With the coordinate representation, one is able to write the matrix elements of $S_{2,outer,i}$ as¹¹

$$\begin{aligned} S_{2,outer,i}^{i'f',if}(r_c) &= \frac{1}{\hbar^2} \int_{-\infty}^{\infty} dt \int_{-\infty}^t dt' \ll i'f', JM_J | \langle L_1(t) L_1(t') \rangle | if, JM_J \gg_{outer,i} \\ &= \frac{\delta_{j_i' j_i} \delta_{f' f}}{\hbar^2 (2j_i + 1)} \int_{-\infty}^{\infty} dt \int_{-\infty}^t dt' \sum_{i_2 m_2} \rho_{i_2} \sum_{m_i} \sum_{i'' m''} \sum_{i'_2 m'_2} e^{i(\omega_{i''} + \omega_{i_2' i_2})t} e^{-i(\omega_{i''} + \omega_{i_2' i_2})t'} \\ &\quad \times \int d\Omega_\alpha \int d\Omega_\beta \langle i' m_i i_2 m_2 | \alpha \rangle V_\alpha(R(t)) \langle \alpha | i'' m'' i'_2 m'_2 \rangle \\ &\quad \times \langle i'' m'' i'_2 m'_2 | \beta \rangle V_\beta(R(t')) \langle \beta | i m_i i_2 m_2 \rangle, \end{aligned} \quad (1)$$

where $\omega_{i''} = [E^{(a)}(i) - E^{(a)}(i'')]/\hbar$, $\omega_{i_2' i_2} = [E^{(b)}(i_2) - E^{(b)}(i_2')]/\hbar$, and $|\alpha\rangle$ is a short notation for $|\delta(\Omega_a - \Omega_{a\alpha})\rangle \otimes |\delta(\Omega_b - \Omega_{b\alpha})\rangle$ and $V_\alpha(R(t))$ represents the potential evaluated at this specified orientation labeled by α . Similarly, one is able to obtain the expression for $S_{2,outer,f}^{i'f',if}(r_c)$ which is the same as Eq. (1) except for making exchanges between the quantum numbers i and f' , between i' and f , and making switches between t and t' . Meanwhile, one can obtain an expression for $S_{2,middle}^{i'f',if}(r_c)$ as¹¹

$$\begin{aligned} S_{2,middle}^{i'f',if}(r_c) &= \frac{1}{\hbar^2} \int_{-\infty}^{\infty} dt \int_{-\infty}^t dt' \ll i'f', JM_J | \langle L_1(t) L_1(t') \rangle | if, JM_J \gg_{middle} \\ &= -\frac{1}{\hbar^2 (2j_i + 1)} \int_{-\infty}^{\infty} dt \int_{-\infty}^{\infty} dt' \sum_{i_2 m_2} \rho_{i_2} \sum_{i'_2 m'_2} \sum_{(m)} e^{i(\omega_{i'} + \omega_{i_2' i_2})t} e^{i(\omega_{f'} + \omega_{i_2' i_2})t'} \\ &\quad \times (-1)^{j_f - m_f + j_f' - m_f'} C(i'f'J, m_i' - m_f' M_J) C(ifJ, m_i - m_f M_J) \\ &\quad \times \int d\Omega_\alpha \int d\Omega_\beta \langle i' m_i' i'_2 m'_2 | \alpha \rangle V_\alpha(\vec{R}(t)) \langle \alpha | i m_i i_2 m_2 \rangle \\ &\quad \times \langle f m_f i_2 m_2 | \beta \rangle V_\beta(\vec{R}(t')) \langle \beta | f' m_f' i'_2 m'_2 \rangle. \end{aligned} \quad (2)$$

It is worth mentioning that as one considers the line coupling occurring among lines within the same bands, expressions for the matrix elements of $S_{2,outer,i}$ and $S_{2,outer,f}$ can be simplified further. It is obvious that among lines within the same bands, both their initial and final vibrational quantum numbers are identical. This implies that one can replace $\delta_{j_i' j_i}$ by $\delta_{i' i}$ in the expression for $S_{2,outer,i}^{i'f',if}(r_c)$ and replace $\delta_{j_f' j_f}$ by $\delta_{f' f}$

in $S_{2,outer,f}^{i'f',if}(r_c)$. As a result, the matrices of both these two terms are diagonal. But, this simplicity does not apply for the matrix of $S_{2,middle}$ which remains as an off-diagonal matrix even within the same bands.

For systems consisting of two linear molecules, formulas used to evaluate the diagonal matrix elements of the $S_{2,outer,i}$, $S_{2,outer,f}$, and $S_{2,middle}$ terms are well known.¹⁰ With respect to

expressions for the off-diagonal matrix elements of $S_{2,\text{middle}}$, a simpler formula applicable for isotropic Raman Q lines with $\omega_{i_i} = \omega_{f_f}$ and a more general one applicable for lines in the P and R branches with $\omega_{i_i} \neq \omega_{f_f}$ are also available.¹¹ However, the more general formula is somehow awkward in practical applications. It becomes desirable to find a more tractable expression.

B. Expression for matrix elements of $S_{2,\text{middle}}$ in the P and R lines

Usually, potential models are given in terms of a spherical tensor expansion as¹⁰

$$V(\vec{R}(t)) = \sum_{L_1 L_2 L} U(L_1 L_2 L; R(t)) \times \sum_{m_1 m_2 m} C(L_1 L_2 L, m_1 m_2 m) Y_{L_1 m_1}(\Omega_a) \times Y_{L_2 m_2}(\Omega_b) Y_{L m}^*(\omega(t)). \quad (3)$$

By inserting this expression for the potential into Eq. (2) and analytically carrying out integrations over the orientations of the two molecules and completing summations over the magnetic quantum numbers as more as possible, one is able to obtain a new expression for the matrix elements of $S_{2,\text{middle}}$ as

$$S_{2,\text{middle}}^{i' f', i f}(r_c) = (-1)^{j_f + j'_f} \sqrt{(2j'_i + 1)(2j'_f + 1)(2j_i + 1)(2j_f + 1)} \times \sum_{L_1 L_2} (-1)^{1+J+L_1} W(j'_i j'_f j_i j_f, J L_1) C(j_i j'_i L_1, 000) C(j'_f j_f L_1, 000) \times \sum_{i_2 i'_2} (2i_2 + 1)(2i'_2 + 1) \rho_{i_2} C^2(i_2 i'_2 L_2, 000) \frac{1}{16\pi^2 \hbar^2 (2L_1 + 1)(2L_2 + 1)} \times \sum_L (-1)^{L_1 + L_2 + L} \sum_M \int_{-\infty}^{\infty} dt \int_{-\infty}^{\infty} dt' e^{i(\omega_{i_i} + \omega_{i'_2})t} e^{-i(\omega_{f_f} + \omega_{i'_2})t'} \times U(L_1 L_2 L; R(t)) U(L_1 L_2 L; R(t')) Y_{LM}^*(\theta_\alpha(t), \phi_\alpha(t)) Y_{LM}(\theta_\beta(t'), \phi_\beta(t')). \quad (4)$$

Then, one can introduce 2D correlation functions defined by

$$G_{L_1 L_2}(t, t') = \frac{1}{16\pi^2 \hbar^2 (2L_1 + 1)(2L_2 + 1)} \sum_L (-1)^{L_1 + L_2 + L} \times U(L_1 L_2 L; R(t)) U(L_1 L_2 L; R(t')) \sum_M Y_{LM}^*(\theta_\alpha(t), \phi_\alpha(t)) Y_{LM}(\theta_\beta(t'), \phi_\beta(t')) = \frac{1}{(4\pi)^3 \hbar^2 (2L_1 + 1)(2L_2 + 1)} \sum_L (-1)^{L_1 + L_2 + L} (2L + 1) \times U(L_1 L_2 L; R(t)) U(L_1 L_2 L; R(t')) P_L(\cos \Theta_{t,t'}), \quad (5)$$

where

$$\cos \Theta_{t,t'} = \cos \theta_\alpha(t) \cos \theta_\beta(t') + \sin \theta_\alpha(t) \sin \theta_\beta(t'). \quad (6)$$

In deriving the above expression, we have assumed that collisional trajectories lie in a half part of the x and z plane with positive x values. As a result, one can simply set $\phi(t) = \phi(t') = 0$. Then, in terms of these 2D correlation functions, the off-diagonal matrix elements of $S_{2,\text{middle}}$ can be expressed as

$$S_{2,\text{middle}}^{i' f', i f}(r_c) = (-1)^{j_f + j'_f} \sqrt{(2j'_i + 1)(2j'_f + 1)(2j_i + 1)(2j_f + 1)} \times \sum_{L_1 L_2} (-1)^{1+J+L_1} W(j'_i j'_f j_i j_f, J L_1) C(j_i j'_i L_1, 000) C(j'_f j_f L_1, 000) \times \sum_{i_2 i'_2} (2i_2 + 1)(2i'_2 + 1) \rho_{i_2} C^2(i_2 i'_2 L_2, 000) \times \int_{-\infty}^{\infty} \int_{-\infty}^{\infty} dt dt' e^{i(\omega_{i_i} + \omega_{i'_2})t} e^{-i(\omega_{f_f} + \omega_{i'_2})t'} G_{L_1 L_2}(t, t'). \quad (7)$$

At this stage, unless $\omega_{i_i} = \omega_{f_f}$, our previous manipulation technique^{10,11} used in deriving the diagonal matrix elements of $S_{2,\text{outer,i}}$, $S_{2,\text{outer,f}}$, and $S_{2,\text{middle}}$ and also in deriving the off-diagonal matrix elements of $S_{2,\text{middle}}$ for isotropic Raman lines

in the Q branch is not applicable. This implies that for lines in the P and R branches, one has to find other approaches. Let us focus attention on the integration part of Eq. (7). By changing its integration variables t and t' to the variables of $\tau \equiv t - t'$ and $\tau' \equiv (1/2)(t + t')$, it can be rewritten as

$$\begin{aligned} & \int_{-\infty}^{\infty} \int_{-\infty}^{\infty} dt dt' e^{i(\omega_{i'i} + \omega_{i_2'i_2})t - i(\omega_{f'f} + \omega_{i_2'i_2})t'} G_{L_1 L_2}(t, t') \\ &= \int_{-\infty}^{\infty} \int_{-\infty}^{\infty} d\tau d\tau' e^{i(\omega_{i'i} + \omega_{i_2'i_2})(\tau' + \frac{\tau}{2}) - i(\omega_{f'f} + \omega_{i_2'i_2})(\tau' - \frac{\tau}{2})} G_{L_1 L_2}\left(\tau' + \frac{\tau}{2}, \tau' - \frac{\tau}{2}\right) \\ &= \int_{-\infty}^{\infty} \int_{-\infty}^{\infty} d\tau d\tau' e^{i\left(\frac{\omega_{i'i} + \omega_{f'f}}{2} + \omega_{i_2'i_2}\right)\tau + i(\omega_{fi} - \omega_{f'i'})\tau'} \mathbb{G}_{L_1 L_2}(\tau, \tau'), \end{aligned} \quad (8)$$

where we have introduced the new 2D symmetric correlation functions defined by

$$\mathbb{G}_{L_1 L_2}(\tau, \tau') = G_{L_1 L_2}\left(\tau' + \frac{\tau}{2}, \tau' - \frac{\tau}{2}\right). \quad (9)$$

It is worth mentioning that in terms of new variables τ and τ' , the original ones are given by $t = \tau' + (1/2)\tau$ and $t' = \tau' - (1/2)\tau$, respectively.

C. Symmetry properties of the 2D correlation functions

It turns out that by exploiting symmetry properties of these new 2D correlation functions, one is able to simplify Eq. (8) further. With respect to the original correlation functions $G_{L_1 L_2}(t, t')$, they have symmetries of $G_{L_1 L_2}(t, t') = G_{L_1 L_2}(t', t)$ and $G_{L_1 L_2}(t, t') = G_{L_1 L_2}(-t, -t')$. The latter represents the fact that collision processes are time-reversal invariant. But, $G_{L_1 L_2}(t, t')$ are neither even functions of t nor even functions of t' . Unfortunately, a failure in pertaining to the evenness for both their two variables t and t' would block their usefulness.

On the other hand, one can conclude that the new correlation functions $\mathbb{G}_{L_1 L_2}(\tau, \tau')$ are invariable for an operation of $\tau \leftrightarrow -\tau$, an operation of $\tau' \leftrightarrow -\tau'$, and an operation for both $\tau \leftrightarrow -\tau$ and $\tau' \leftrightarrow -\tau'$. The first two properties mean they become even functions both over τ and τ' . The last one represents the fact that collisional processes are time-reversal invariant. The above conclusions are based on the symmetry properties of the functions of $G_{L_1 L_2}(\tau' + \frac{\tau}{2}, \tau' - \frac{\tau}{2})$,

$$\begin{aligned} & G_{L_1 L_2}\left(\tau' + \frac{\tau}{2}, \tau' - \frac{\tau}{2}\right) \\ &= G_{L_1 L_2}\left(\tau' - \frac{\tau}{2}, \tau' + \frac{\tau}{2}\right) \\ &= G_{L_1 L_2}\left(-\tau' + \frac{\tau}{2}, -\tau' - \frac{\tau}{2}\right) \\ &= G_{L_1 L_2}\left(-\tau' - \frac{\tau}{2}, -\tau' + \frac{\tau}{2}\right). \end{aligned} \quad (10)$$

Meanwhile, in contrast with $G_{L_1 L_2}(t, t')$, $\mathbb{G}_{L_1 L_2}(\tau, \tau')$ do not have a symmetry between τ and τ' . In other words, they vary

differently as τ and τ' vary. It is worth mentioning that all these 2D correlation functions are associated with specified collisional trajectories. Usually, the latter are labeled by the closest distance r_c (or the impact parameter b). As a result, they are also functions of r_c . For simplicity, this dependence may not explicitly be presented.

As example, we consider the $C_2H_2-N_2$ pair in the present study. If one assumes no bending modes of the C_2H_2 molecule are excited and only considers its stretching bands, this molecule remains linear. Thus, all the formulas developed above are applicable for this system. Besides, a new potential model containing 85 spherical components labeled by combinations of even values of the tensor ranks L_1 , L_2 , and L is available recently in the literature.¹⁵ Based on this potential model, one can calculate the original 2D correlation functions $G_{L_1 L_2}(t, t')$ associated with a specified selection of L_1 and L_2 and the newly introduced ones $\mathbb{G}_{L_1 L_2}(\tau, \tau')$. In practical calculations, instead of t and t' people prefer to use dimensionless variables $z \equiv vt/r_c$ and $z' \equiv v't'/r_c$, where v is the averaged velocity for the “exact” trajectory model and is the “apparent” velocity for the “parabolic” trajectory model.⁵ We follow this common custom here.

Thus, there are two sets of variables used in the present study. One set consists of variables with dimensions that appear in formulas and another set consists of dimensionless variables which appear in plots. Within the first set, there are original t and t' and new introduced τ and τ' . Within the dimensionless set, there are z and z' corresponding to t and t' , and there are $u \equiv v\tau/r_c$ and $v \equiv v'\tau'/r_c$ corresponding to τ and τ' . It is obvious that $u = z - z'$ and $v = (z + z')/2$. For simplifying notations, we use the same function symbol for $G_{L_1 L_2}(t, t')$ and $G_{L_1 L_2}(z, z')$, and the same symbol for $\mathbb{G}_{L_1 L_2}(\tau, \tau')$ and $\mathbb{G}_{L_1 L_2}(u, v)$. In order to avoid confusion, we list notations used in the present study in Table I.

In order to show profiles of $G_{L_1 L_2}(z, z')$ and $\mathbb{G}_{L_1 L_2}(u, v)$, we consider their most important components associated with $L_1 = 2$ and $L_2 = 0$ and present their three dimensional profiles obtained at $r_c = 4.5 \text{ \AA}$ in Figs. 1 and 2, respectively. To choose $r_c = 4.5 \text{ \AA}$ as an example mainly results from a fact that the profiles at this region contain more structures and their profile

TABLE I. Notations used in the present study.

Variables with dimension		Dimensionless variables	
Correlation functions	Fourier transforms	Correlation functions	Fourier transforms
$G_{L_1L_2}(t, t')$		$G_{L_1L_2}(z, z')$	
$\mathbb{G}_{L_1L_2}(\tau, \tau')$, where $\tau = t - t'$ and $\tau' = (t + t')/2$	$\mathbb{F}_{L_1L_2}(\omega, \omega')$	$\mathbb{G}_{L_1L_2}(u, v)$, where $u = z - z'$ and $v = (z + z')/2$	$\mathbb{F}_{L_1L_2}(k, k')$

differences can be more clearly exhibited. As shown in Fig. 1, $G_{20}(z, z')$ is neither even over z nor even over z' . In contrast, $\mathbb{G}_{20}(u, v)$ becomes an even function over both u and v .

D. The 2D Fourier transforms of the 2D correlation functions

Because $\mathbb{G}_{L_1L_2}(\tau, \tau')$ become even functions of τ and τ' , their Fourier transforms are real. One can introduce their 2D

Fourier transforms defined by

$$\mathbb{F}_{L_1L_2}(\omega, \omega') = \frac{1}{2\pi} \int_{-\infty}^{\infty} \int_{-\infty}^{\infty} d\tau d\tau' e^{i\omega\tau} e^{i\omega'\tau'} \mathbb{G}_{L_1L_2}(\tau, \tau'). \quad (11)$$

Then, in terms of these Fourier transforms, one is able to rewrite Eq. (8) as

$$\begin{aligned} & \int_{-\infty}^{\infty} \int_{-\infty}^{\infty} d\tau d\tau' e^{i\left(\frac{\omega_{i'1} + \omega_{f'1}}{2} + \omega_{i'2}\right)\tau + i(\omega_{f1} - \omega_{f'1})\tau'} \mathbb{G}_{L_1L_2}(\tau, \tau') \\ &= \frac{1}{2\pi} \int_{-\infty}^{\infty} \int_{-\infty}^{\infty} d\tau d\tau' e^{i\left(\frac{\omega_{i'1} + \omega_{f'1}}{2} + \omega_{i'2}\right)\tau + i(\omega_{f1} - \omega_{f'1})\tau'} \int_{-\infty}^{\infty} \int_{-\infty}^{\infty} d\omega d\omega' e^{-i\omega\tau} e^{-i\omega'\tau'} \mathbb{F}_{L_1L_2}(\omega, \omega') \\ &= \frac{1}{2\pi} \int_{-\infty}^{\infty} \int_{-\infty}^{\infty} d\omega d\omega' \mathbb{F}_{L_1L_2}(\omega, \omega') \int_{-\infty}^{\infty} \int_{-\infty}^{\infty} d\tau d\tau' e^{i\left(\frac{\omega_{i'1} + \omega_{f'1}}{2} + \omega_{i'2} - \omega\right)\tau + i(\omega_{f1} - \omega_{f'1} - \omega')\tau'} \\ &= \frac{1}{2\pi} \int_{-\infty}^{\infty} \int_{-\infty}^{\infty} d\omega d\omega' \mathbb{F}_{L_1L_2}(\omega, \omega') \delta\left(\omega - \frac{\omega_{i'1} + \omega_{f'1}}{2} - \omega_{i'2}\right) \delta(\omega' - \omega_{f1} + \omega_{f'1}) \\ &= 2\pi \mathbb{F}_{L_1L_2}\left(\frac{\omega_{i'1} + \omega_{f'1}}{2} + \omega_{i'2}, \omega_{f'1} - \omega_{f1}\right). \end{aligned} \quad (12)$$

Finally, in terms of these 2D Fourier transforms $\mathbb{F}_{L_1L_2}(\omega, \omega')$, the off-diagonal matrix elements of $S_{2,\text{middle}}$ can be simplified as

$$\begin{aligned} S_{2,\text{middle}}^{i'f',i'f}(r_c) &= 2\pi(-1)^{j_f+j'_f} \sqrt{(2j'_i+1)(2j'_f+1)(2j_i+1)(2j_f+1)} \\ &\quad \times \sum_{L_1L_2} (-1)^{1+J+L_1} W(j'_i j'_f j_i j_f, JL_1) C(j_i j'_i L_1, 000) C(j'_f j_f L_1, 000) \\ &\quad \times \sum_{i_2 i'_2} (2i_2+1)(2i'_2+1) \rho_{i_2} C^2(i_2 i'_2 L_2, 000) \mathbb{F}_{L_1L_2}\left(\frac{\omega_{i'1} + \omega_{f'1}}{2} + \omega_{i'_2}, \omega_{f'1} - \omega_{f1}\right). \end{aligned} \quad (13)$$

In comparison with the general expression derived in our previous study¹¹ and other formulas available in literature,²⁰ Eq. (13) has several advantages. First of all, this expression is more concise. Besides, because the 2D Fourier transforms $\mathbb{F}_{L_1L_2}(\omega, \omega')$ are real, one can easily draw a conclusion that the off-diagonal elements of $S_{2,\text{middle}}$ are real too. In contrast, with other formulas, to verify the above conclusion is not such straightforward because in general, they contain complex functions. However, the most advantage in usage of Eq. (13) is that the number of functions $\mathbb{F}_{L_1L_2}(\omega, \omega')$ is very limited. As example, for the system of $C_2H_2-N_2$, by using

Eq. (13) one only needs to evaluate six 2D Fourier transforms labeled by L_1 and L_2 as (20), (22), (24), (40), (42), and (44). In practical calculations, in order to simplify further, one can omit three minor ones with (24), (42), and (44). It is well known that as long as the “exact” trajectory model is adopted in calculations, all the functions introduced such as those resonance functions appearing in literature have to be numerically evaluated. If one uses other formulas to calculate the off-diagonal matrix elements of $S_{2,\text{middle}}$, the number of these functions would increase dramatically. In addition, they are complex functions.

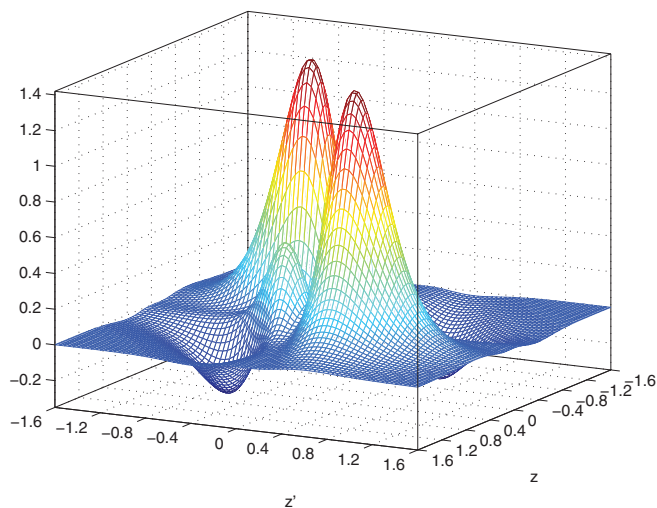


FIG. 1. The 2D correlation function of $G_{20}(z, z')$ (in ps^{-2}) at $T = 296$ K and $r_c = 4.5$ Å for a molecular pair of $\text{C}_2\text{H}_2\text{-N}_2$. The calculation is based on the new potential model¹⁵ and the “exact” trajectory model.

It is interesting to note that there is a simple relation between the 2D correlation functions and their one dimensional (1D) partners introduced previously¹⁰ in calculating the diagonal matrix elements of $S_{2,\text{outer},i}$, $S_{2,\text{outer},f}$, and $S_{2,\text{middle}}$. With the current notations, the 1D correlation functions introduced previously are defined as

$$G_{L_1L_2}(\tau) = \int_{-\infty}^{\infty} d\tau' \mathbb{G}_{L_1L_2}(\tau, \tau'). \quad (14)$$

Similarly, there is also a simple relation between the 2D Fourier transforms $\mathbb{F}_{L_1L_2}(\omega, \omega')$ and the 1D Fourier transforms $F_{L_1L_2}(\omega)$ which is defined by

$$F_{L_1L_2}(\omega) = \frac{1}{\sqrt{2\pi}} \int_{-\infty}^{\infty} d\tau e^{i\omega\tau} G_{L_1L_2}(\tau). \quad (15)$$

Because ω corresponds to τ and the latter represents the gap between t and t' , it becomes clear that it is how the original 2D correlation functions $G_{L_1L_2}(t, t')$ vary with $t - t'$ that matters at the last stage of calculations for the diagonal matrix elements of $S_{2,\text{outer},i}$, $S_{2,\text{outer},f}$, and $S_{2,\text{middle}}$.

Finally, it is easy to find out that

$$\begin{aligned} \mathbb{F}_{L_1L_2}(\omega, 0) &= \frac{1}{2\pi} \int_{-\infty}^{\infty} d\tau e^{i\omega\tau} \int_{-\infty}^{\infty} d\tau' \mathbb{G}_{L_1L_2}(\tau, \tau') \\ &= \frac{1}{2\pi} \int_{-\infty}^{\infty} d\tau e^{i\omega\tau} G_{L_1L_2}(\tau) \\ &= \frac{1}{\sqrt{2\pi}} F_{L_1L_2}(\omega). \end{aligned} \quad (16)$$

As a result, it becomes obvious that the expression for the off-diagonal matrix elements of $S_{2,\text{middle}}$ is also applicable for its diagonal matrix elements.

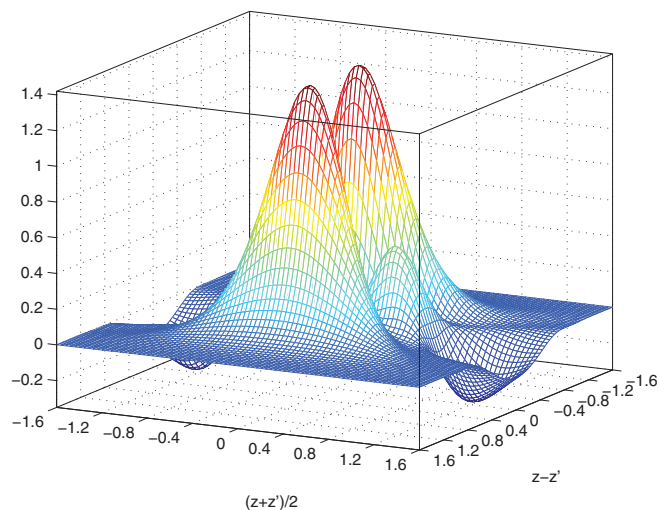


FIG. 2. The same as Fig. 1 except for the 2D correlation function of $\mathbb{G}_{20}(u, v)$.

E. Tools used in numerical calculations

In practice, the success in applying the new method to calculate these off-diagonal matrix elements of $S_{2,\text{middle}}$ relies on how to effectively and accurately evaluate these 2D Fourier transforms. Thanks to our experiences in calculating pressure broadened half-widths and induced shifts, we have accumulated enough tools to overcome this challenge. First of all, by introducing the coordinate representation, the main calculation task is reduced to calculate the 2D correlation functions and their 2D Fourier transforms. As mentioned above, the number of these functions is very limited. In addition, as shown in Eq. (5), no matter how complicated the potential model used would be, there is no any difficulty to evaluate these 2D correlation functions accurately.

Second, in our previous studies we have developed an effective approach to derive 1D Fourier transforms. This method is based on the sampling theory.²¹ The basic idea is by sampling, one converts a function of interest to a sequence in the time domain, calculates its discrete Fourier transform with the fast Fourier transforms (FFT),²² and then relates this transformed sequence in the frequency domain to the Fourier transform of the original function.

When we try to extend our study on the line coupling from Raman Q lines into infrared P and R lines, we have faced a challenge how to evaluate a 2D Fourier transform from a 2D correlation function. Fortunately, in other scientific and engineering fields such as the signal theory¹⁴ to deal with data processing and analysis, to consider the 2D Fourier transforms of the 2D functions is a familiar subject. There are many books and papers in literature and there are several tools available there with which one can compute the 2D Fourier transforms. For example, it has been known that the 2D Fourier transform is linearly separable: the Fourier transform of a 2D image is the Fourier transform of the rows followed by the Fourier transforms of the resulting columns (or vice versa). Based on this fact, the 2D Fourier transform can be carried out by 1D Fourier transforming all the rows of the 2D signal and then 1D Fourier transforming all the columns of the resulting matrix. In the present study, because we have very effective programs

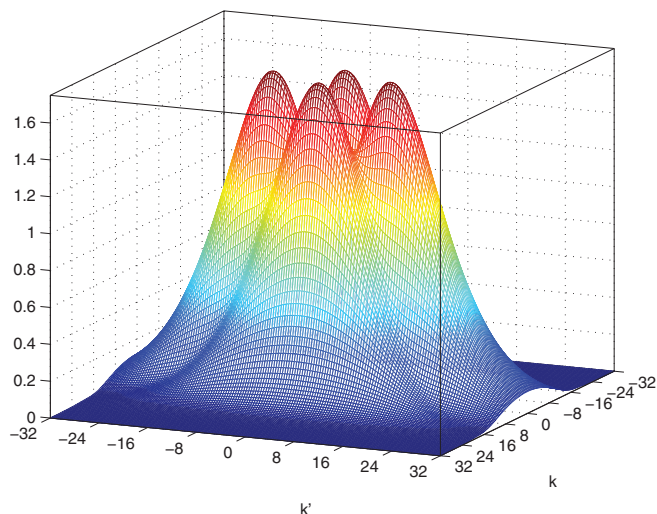


FIG. 3. The 2D Fourier transform $\mathbb{F}_{20}(k, k')$ (in ps^{-2}) at $T = 296$ K for a molecular pair of $\text{C}_2\text{H}_2\text{-N}_2$. The calculation is based on the “exact” trajectory model with $r_c = 4.0$ Å.

to carry out the 1D Fourier transform, we have adopted this straightforward way to compute the 2D Fourier transform and have obtained satisfactory results.

Based on the new potential model,¹⁵ one can find the minimum of the closest distance for the “exact” trajectories at $T = 296$ K is $r_{c,\text{min}} = 3.7546$ Å. Because nearly head-on collisions play a dominant role in the line coupling, we select a trajectory with $r_c = 4.0$ Å as example. Among all the components, we consider the most important one with $L_1 = 2$ and $L_2 = 0$. Again, we prefer to plot functions with dimensionless arguments used in our numerical calculations. In this case, the function is $\mathbb{F}_{20}(k, k')$ which is the Fourier transform of $\mathbb{G}_{20}(u, v)$. Thus, we present the three dimensional

plot of $\mathbb{F}_{20}(k, k')$ obtained at $r_c = 4.0$ Å in Fig. 3. This plot provides a whole picture about how its magnitudes vary with its two variables k and k' at this specified trajectory.

In order to more clearly provide some numerical measures on magnitudes of $\mathbb{F}_{20}(k, k')$, we present another plot to show its profiles as functions of k or k' with three fixed k' or k values of 0.0, 8.0, and 16.0 in Fig. 4. By combining Figs. 3 and 4, one can find that in terms of the coordinates of k and k' , there are four peaks with their heights at $(0, 10)$, $(0, -10)$, $(5, 0)$, and $(-5, 0)$. The first two peaks are symmetrically located at k' axis and the last two are symmetrically at k axis. In addition, the former’s height is almost identical to the latter’s height. But, shapes of the peaks in different pairs are quite different. In general, the peaks in the first pair distribute more widely than those in the second pair. As shown in Fig. 4, roughly speaking after $k > 15$, magnitudes of $\mathbb{F}_{20}(k, k')$ would decrease more than one order from its maximum. On the other hand, its magnitudes could still remain significant or non-negligible as long as $k' < 30$. We will be back to this subject later.

III. CALCULATIONS OF HALF-WIDTHS FOR C_2H_2 LINES BROADENED BY N_2

A. Half-widths of isotropic Raman Q lines

First of all, we present our calculated half-widths for isotropic Raman Q lines of C_2H_2 broadened by N_2 obtained from including the line coupling. The calculation is similar to that reported in our previous work for N_2 lines broadened by N_2 .¹¹ Here, we briefly outline some of main factors to determine effects from the line coupling. First of all, let us look at the dashed-dotted black curve with $k' = 0$ in Fig. 4. After reaching its maximum at $k = 5$, magnitudes of this curve

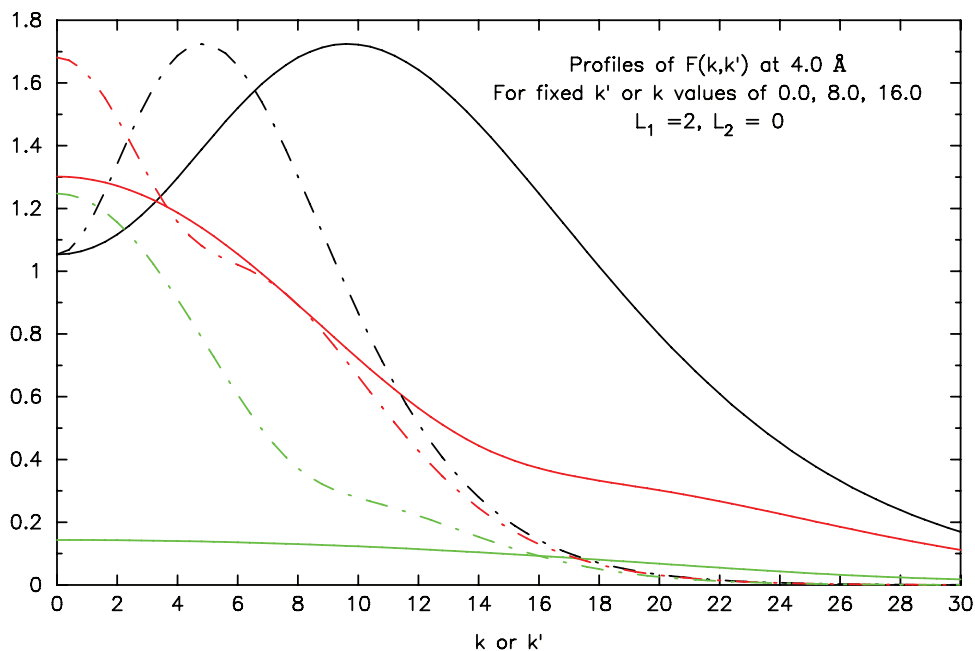


FIG. 4. $\mathbb{F}_{20}(k, k')$ (in ps^{-2}) at $r_c = 4.0$ Å and $T = 296$ K with three fixed k' values as functions of k , plotted by three dashed-dotted curves. Meanwhile, $\mathbb{F}_{20}(k, k')$ as function of k' with three fixed k values are plotted by three solid curves. The black, red, and green colors correspond to the three fixed values of 0.0, 8.0, and 16.0.

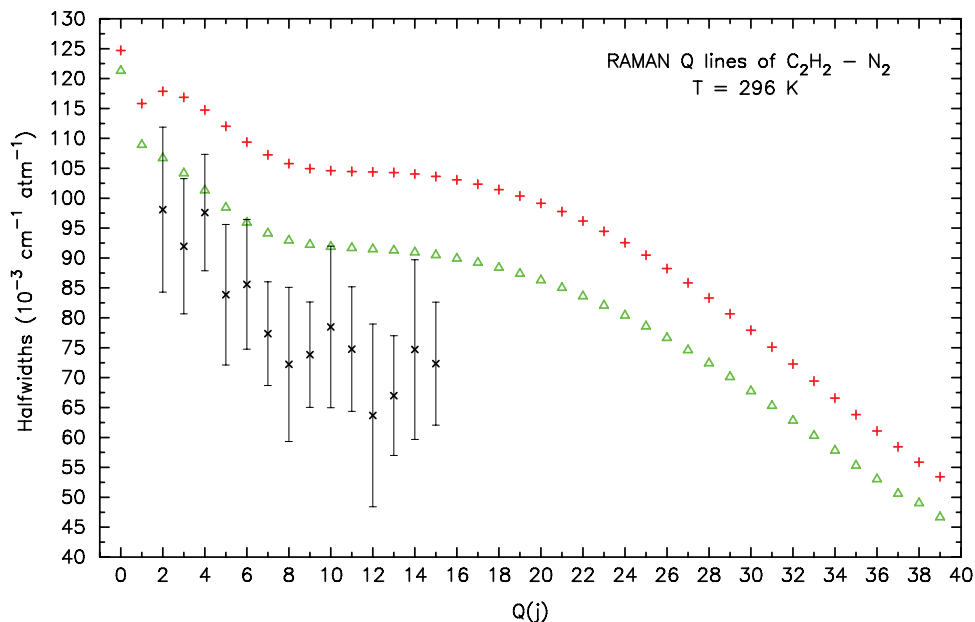


FIG. 5. Comparison of calculated half-widths at 296 K for the isotropic Raman Q lines of C_2H_2 broadened by N_2 . Theoretically calculated results from the modified RB formalism without and with the line coupling are plotted by + (red) and Δ (green), respectively. Meanwhile, measured values at 298 K²³ are given by \times .

decrease as k increases, but still remain significant within a range of $k < 14$. This curve represents the profile of $F_{20}(k, 0)$ and the latter is associated with $F_{20}(\omega, 0) (= \frac{1}{\sqrt{2\pi}} F_{20}(\omega))$. For the specified conditions of the plot (i.e., $r_c = 4.0 \text{ \AA}$ and $T = 296 \text{ K}$), the value convert from ω (in cm^{-1}) to k (dimensionless) is $k \approx 0.11 \times \omega$. Thus, we know that as long as the first argument of $F_{20}(\omega_{i_1} + \omega_{i_2}, 0)$ in Eq. (13) is less than 127 cm^{-1} , one has to consider the line coupling. On the other hand, the rotational constant B of the C_2H_2 molecule is only around 1.2 cm^{-1} . This implies that for the most nearby coupled lines, their initial (or final) energy gaps together with

$\omega_{i_2 i_1}$ are well within this argument range to make contributions to the off-diagonal matrix elements of $S_{2, \text{middle}}$.

Based on these facts, one can expect that effects on calculated half-widths of C_2H_2 immersed in N_2 bath would be significant. In Figs. 5 and 6, we present our calculated values by considering the line coupling at $T = 296 \text{ K}$ and $T = 150 \text{ K}$, respectively, together with those derived from the modified RB formalism without taking into account the line coupling. As comparisons, recent measured data²³ at $T = 298 \text{ K}$ and $T = 150 \text{ K}$ are also plotted in these figures. As shown in Figs. 5 and 6, by taking into account the line coupling, the new

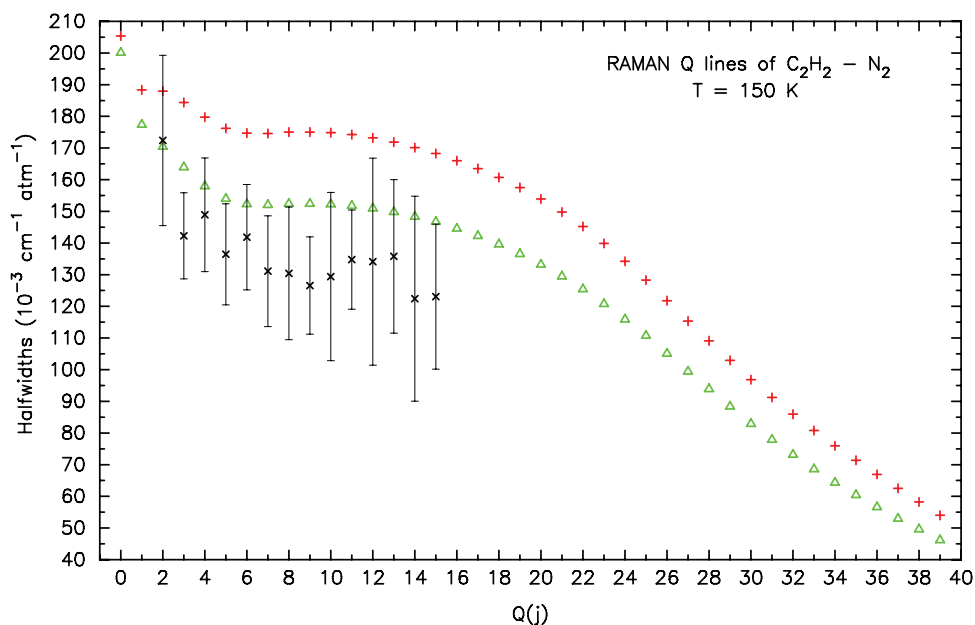


FIG. 6. The same as Fig. 5 except that calculations and measurements²³ are carried out at 150 K.

TABLE II. Energy and frequency values for coupled P and R lines.

Lines	P(j-2) j-3 ← j-2	R(j-2) j-1 ← j-2	P(j) j-1 ← j	R(j) j+1 ← j	P(j+2) j+1 ← j+2	R(j+2) j+3 ← j+2
E_f and E_i (in B)	(j-3)(j-2), (j-2)(j-1)	(j-1)j, (j-2)(j-1)	(j-1)j, j(j+1)	(j+1)(j+2), j(j+1)	(j+1)(j+2), (j+2)(j+3)	(j+3)(j+4), (j+2)(j+3)
ω_{fi} (in B)	-2(j-2)	2(j-1)	-2j	2(j+1)	-2(j+2)	2(j+3)

calculated values at 296 K and 150 K are reduced by about 13% and 14%, respectively, and they become closer to the measured values. Thus, one can conclude that it is absolutely necessary to consider the line coupling in calculating N_2 broadened half-widths of isotropic Raman Q lines of the C_2H_2 molecule.

B. Half-widths of infrared P and R lines

In this section, by considering infrared P and R lines of C_2H_2 immersed in the N_2 bath, we present some things new. We would like to mention that we have adjusted our practical calculations to match the potential model adopted.¹⁵ First of all, we provide some facts. It has been known that for lines within the same bands, the $S_{2,outer,i}$ and $S_{2,outer,f}$ terms are diagonal and their diagonal matrix elements are complex. Usually, $ImS_{2,outer,i}$ and $ImS_{2,outer,f}$ are one order smaller than $ReS_{2,outer,i}$ and $ReS_{2,outer,f}$. Meanwhile, the $S_{2,middle}$ term is always off-diagonal, but all its matrix elements are real. Finally, the iS_1 term is imaginary and it is the main component of ImS . If the potential models do not have vibrational dependences, iS_1 becomes zero.

Because the current potential model¹⁵ does not have vibrational dependences, we are not able to properly evaluate the iS_1 term at all. This deficiency would cause a large uncertainty in evaluating the whole ImS . Based on this and the other fact mentioned above, we have decided to completely ignore the whole ImS ($=iS_1 + ImS_{2,outer,i} + ImS_{2,outer,f}$) in our practical calculations.

Before presenting our final results, we would like to provide estimation of how important the effects from the line coupling would be. The effects are mainly determined by that in comparison with the whole diagonal matrix elements of ReS_2 , whether the off-diagonal matrix elements of $S_{2,middle}$ given by Eq. (13) are significant or not. By analyzing the profiles of 2D Fourier transforms $\mathbb{F}_{L_1L_2}(\omega, \omega')$ and considering their two arguments of $\frac{\omega_{i'1} + \omega_{f'f}}{2} + \omega_{i_2' i_2}$ and $\omega_{f'f} - \omega_{fi}$ appearing in Eq. (13), one can find the answer. First of all, because there is no Q branch in stretching bands, one only needs to consider P and R lines. Second, two coupled lines must share the same parity for their initial angular quantum numbers. The same conclusion is also true for their final quantum numbers.

Based on the evenness of the tensor rank L_1 , the whole line space constructed by all the P and R lines can be divided into two independent sub-spaces. One consists of R(0), P(2), R(2), P(4), R(4), ... and another consists of P(1), R(1), P(3), R(3), and so on. Then, lines only in the same groups can be coupled. We list general expressions for their initial and final rotational energies together with their frequency excluding vibrational band center for lines in the same groups in Table II. With Table II, one can find corresponding averaged energy gaps ($=\frac{\omega_{i'1} + \omega_{f'f}}{2}$) and frequency gaps ($=\omega_{f'f} - \omega_{fi}$) between coupled lines. Besides, the general expressions for these two quantities are presented in Table III.

As shown in Table III, the frequency gaps between two coupled nearby R lines are constant (i.e., $\pm 4.8 \text{ cm}^{-1}$). In contrast, the frequency gaps between two coupled nearby P and R lines are $\pm 2(2j+1)$ and $\pm 2(2j+3)$ which increase very quickly as j increases. We note that after making the variable exchange, this argument appears as k' in the 2D Fourier transforms $\mathbb{F}_{L_1L_2}(k, k')$. For the specified trajectory with $r_c = 4.0 \text{ \AA}$, $\omega = 4.8 \text{ cm}^{-1}$ corresponds to $k = 0.53$ which is pretty small. Then, roughly speaking, contributions to the line coupling between two nearby R lines are mainly determined by profiles of $\mathbb{F}_{L_1L_2}(k, 0)$. Among them, the profile of their major component $\mathbb{F}_{20}(k, 0)$ is given by the dashed-dotted black line in Fig. 4. In contrast, contributions to the line coupling between two nearby P and R lines are from other $\mathbb{F}_{L_1L_2}(k, k')$ with $k' > 0$ whose magnitudes are smaller than $\mathbb{F}_{L_1L_2}(k, 0)$. The larger the j value is, the larger the k' is and the smaller the contributions are. Therefore, one can expect that in each of these two sub-spaces, especially for lines with large j values, the line couplings mainly occur among lines within the same branches. In other words, in comparison with the couplings within the same branches, except for lines with small j values, the line couplings between the P and R branches are not important. Our numerical calculations shown later have verified this expectation. This result was also previously obtained from fully quantum calculations of line mixing effect in CO-He.¹⁸

For each of selected 600 values of r_c ranging from $r_{c,min}$ to 40.0 \AA , we have calculated all the diagonal and off-diagonal matrix elements of $S_2(r_c)$ in the sub-space constructed by coupled lines of R(0), P(2), R(2), ..., P(40), R(40), and P(42). The size of these matrices is 42×42 which is large enough,

TABLE III. Averaged energy gaps and frequency gaps between coupled nearby lines.

Coupled lines	R(j-2) ~ R(j)	P(j) ~ R(j)	P(j+2) ~ R(j)	R(j+2) ~ R(j)
Energy gap (in B)	$\pm 4j$	$\pm(2j+1)$	$\pm(2j+3)$	$\pm 4(j+2)$
Frequency gap (in B)	± 4	$\pm 2(2j+1)$	$\pm 2(2j+3)$	± 4

but remains tractable. Because we have set 4 as the upper limit of L_1 , these $S_2(r_c)$ become five diagonal matrices. In addition, they are real and asymmetric. With the same method developed in our previous work,¹¹ we can find the matrices of $\exp[-S_2(r_c)]$. After the latter are available, by using the expression for matrix elements of the relaxation matrix W given by

$$W^{i'f',if} = \frac{n_b v}{2\pi c} \int_{r_{c,min}}^{+\infty} 2\pi \left(b \frac{db}{dr_c} \right) dr_c \times \{ \delta_{i'i} \delta_{f'f} - \ll i'f' | e^{-S_2(r_c)} | if \gg \}, \quad (17)$$

one can easily derive all the matrix elements of the relaxation operator W whose diagonal matrix elements correspond to the calculated half-widths with including effects from the

line coupling. The results are presented in Matrix 1 where due to lack of room to print all its contents, some rows and columns are removed. As shown in Matrix 1, the W matrix has large and positive diagonal elements representing the corresponding half-widths. With respect to its off-diagonal elements, those corresponding to the line mixing within the same branches (i.e., the P-P and R-R mixings) are negative and that associated with the line mixing between two different branches (i.e., the P-R and R-P mixings) are positive. In other words, in comparison with the P-P and R-R mixing terms, the P-R and R-P mixing terms have an opposite sign, as also previously observed for CO-He.¹⁸ In addition, the former's magnitudes are significantly larger than the latter's. This feature results from the fact that the line couplings within the same branches are more important than that happening between different branches.

Matrix 1: A 42×42 matrix of the relaxation operator W in the P and R line space

122.064	7.265	-10.247	2.984	-3.739	2.072	-2.454	1.583	-1.790	·	-0.003	0.001
7.216	115.901	4.528	-12.931	2.876	-5.121	2.213	-3.391	1.751	·	0.003	-0.002
-10.077	4.482	112.361	3.528	-13.935	2.645	-5.969	2.128	-3.987	·	-0.005	0.002
2.896	-12.614	3.483	109.017	2.982	-14.047	2.404	-6.467	1.999	·	0.004	-0.004
-3.562	2.773	-13.452	2.941	105.603	2.607	-13.935	2.192	-6.762	·	-0.008	0.002
1.951	-4.798	2.541	-13.362	2.570	102.418	2.323	-13.926	2.020	·	0.004	-0.006
-2.247	2.072	-5.488	2.306	-12.998	2.290	99.803	2.103	-14.191	·	-0.011	0.003
1.443	-3.036	1.988	-5.816	2.102	-12.689	2.074	97.896	1.933	·	0.004	-0.008
-1.577	1.595	-3.486	1.870	-5.934	1.939	-12.606	1.907	96.603	·	-0.016	0.003
·	·	·	·	·	·	·	·	·	·	·	·
-0.001	0.001	-0.002	0.001	-0.003	0.001	-0.004	0.002	-0.005	·	46.968	0.037
0.000	-0.000	0.001	-0.001	0.001	-0.002	0.001	-0.003	0.001	·	0.034	44.758

Similarly, we have calculated the matrix elements of W in the sub-space constructed by other coupled lines of P(1), R(1), P(3), ..., R(39), P(41), and R(41). It turns out that because the vibrational dependences have not been taken into account, this W matrix is identical to the previous one. As a result, one can identify the half-widths not only for all the even R lines, but also for all odd R lines from Matrix 1 alone because the half-width of $2j \leftarrow 2j - 1$ (i.e., R($2j - 1$)) is the same as $2j - 1 \leftarrow 2j$ (i.e., P($2j$)) with the rigid rotor approximation.¹⁹

After all these values are available, we present the calculated half-widths of the R lines obtained from considering all possible line couplings within all P and R lines together with those derived from the modified RB formalism without the line coupling in Fig. 7. For comparison, some measured values¹⁶ are also plotted. As shown in the figure, values obtained from the RB formalism significantly overestimate the

half-widths of the R lines of C_2H_2 broadened by N_2 . This demonstrates a known fact that the RB formalism predicts too large amounts of the half-width for two linear molecular systems. Meanwhile, after considering the line coupling, the new formalism can significantly reduce calculated half-widths by amounts as large as 13%. Although, in comparison with measurements, there are still large gaps existing, but the refinement goes in the right direction. This conclusion has been found in our previous study on the isotropic Raman Q lines of N_2 broadened by N_2 and it is confirmed here again.

Furthermore, in order to show the line coupling within the same branches plays a dominant role in determining its effects on calculated half-widths, we have also calculated the W matrix without including the line coupling between the P and R branches and present the calculated results in Fig. 7. As shown in the figure, the differences between these two results

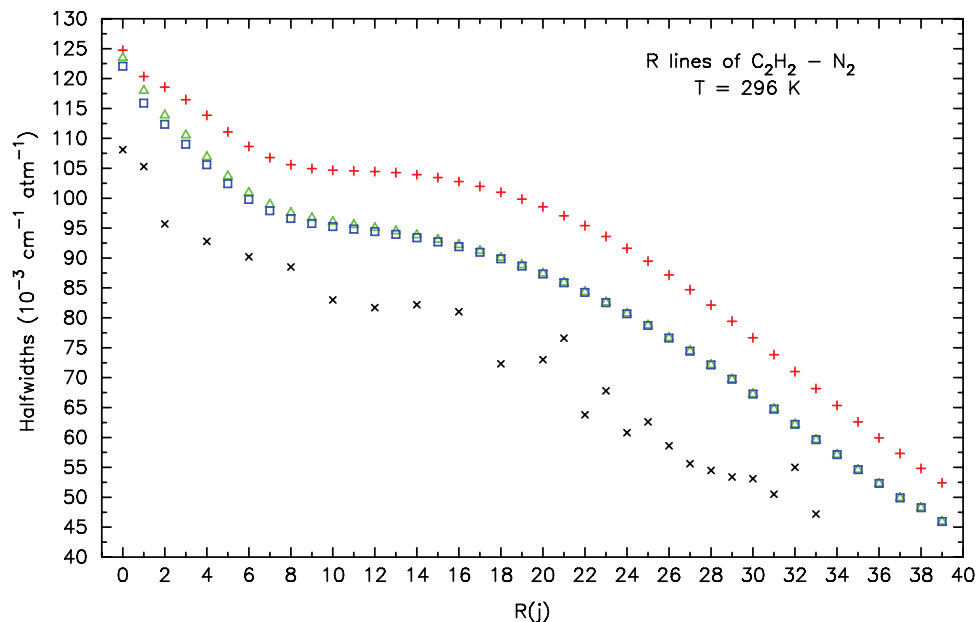


FIG. 7. Comparison of calculated half-widths of the infrared R lines for C_2H_2 broadened by N_2 derived from with and without taking into account effects from the line coupling. They are represented by \square (blue) and $+$ (red), respectively. Meanwhile, some measured data¹⁶ are plotted by \times . In addition, theoretically calculated half-widths of the R lines by neglecting inter-branch coupling are plotted by (green).

are small. More specifically, all the differences are less than 2% and after $j \geq 8$, they become less 1%. Therefore, one can conclude that to ignore the line coupling between the P and R branches is a good approximation for this system. To isolate the R lines from the P lines would reduce the size of the S_2 matrices by a half, but it can still yield good results. In the present study, because the size of S_2 (i.e., 42×42) remains well tractable, one does not need to rely on this simplification. But, it is worth to mention it here.

IV. DISCUSSIONS AND CONCLUSIONS

First of all, we would like to compare our new method with approaches used by others. It is well known that people have developed several formalisms to consider the line coupling for different molecular systems. Among them, Cherkasov has spent more than three decades to study this subject²⁰ and one of his papers appears recently.²⁴ In our previous study,¹¹ we have provided a detailed comparison of his method and ours. Meanwhile, there are two recent papers by Starikov.^{25,26} In the first paper, the author has introduced so called bi-resonance functions in the theory of collisional broadening of the spectral lines of molecules to consider the line interference. He has provided comprehensive lists of the forms with which these bi-resonance functions associated with the straight-line, the parabolic, and the “exact” trajectories can be modeled. In the second one, with the bi-resonance functions he has considered overlapping lines of the ammonia molecule broadened by argon and helium.

It is worth mentioning that there is no essential difference between Starikov’s bi-resonance functions defined as summations of products of resonance functions and their partners’ complex conjugates over the magnetic quantum numbers and those resonance products appearing in Cherkasov’s formulas.

In addition, the two same arguments (i.e., the initial energy gap and the final energy gap of the two coupled lines) serve as the two modulation frequencies in both these resonance forms. Of course, Cherkasov only considers simpler potential and trajectory models and Starikov covers more models. With respect to a more profound problem resulting from how to diagonalize matrices with a large size at each step in averaging over the states of the bath molecule, Starikov has completely followed the approach by Cherkasov. As explained in our previous work,¹¹ by correctly applying the cumulant expansion, one is able to dramatically reduce the size of matrices to be diagonalized. As a result, an extra approximation introduced by Cherkasov to separate the relaxation operators into one diagonal part and another off-diagonal part becomes unnecessary.

Furthermore, by fully exploiting the coordinate representation, the 2D correlation functions can be introduced and by making variable changes these functions become even. Then, the latter’s 2D Fourier transforms are real and the complexity resulting from involving complex functions in calculating the off-diagonal matrix elements is completely obviated in advance. In addition, in comparison with others’ formalism given in terms of the bi-resonance functions and the products of resonance functions, contributions from one specified 2D Fourier transform $\mathbb{F}_{L_1 L_2}(\omega, \omega')$ alone in our formalism correspond to a combination of contributions from a whole group of those resonance forms. The group categorized by the common rotational symmetry labels of L_1 and L_2 consists of a lot of the resonance forms having different other indices, including those used to distinguish different R dependences. This implies that with our formalism, we are able to dramatically reduce the number of these functions. In fact, we believe that the number has been reduced to the minimum. Finally, the two modulation frequencies of these 2D Fourier transforms represent real intrinsic connections between two coupled lines. All these features uniquely exist in our new formalism.

Concerning with our numerically calculated half-widths of both the isotropic Raman Q lines and the infrared P and R lines for C_2H_2 broadened by N_2 , the conclusion is that effects from the line coupling are important. This conclusion is well expected because the C_2H_2 molecule has a small rotational constant. In general, in comparison with that derived from the modified RB formalism, calculated half-widths with the line coupling are reduced by 12%–14% and become closer to measurements.

However, if one investigates the whole relaxation matrix W further, one needs to verify the detailed balance principle (which connects the elements of $W^{i'f',if}$ and $W^{if,i'f'}$) and the sum rule²⁷ (which connects the diagonal and off-diagonal elements of W). For the isotropic Raman spectra of N_2 , these properties were recently studied and the limits of a semi-classical treatment were analyzed.²⁸ A similar study for the infrared spectra is under development.

Finally, we would like to mention some procedures that have not been taken into account in the present study. Because the current potential model does not contain any vibrational dependence, we are not able to meaningfully calculate the imaginary term iS_1 which is a main component of the imaginary part of $iS_1 + S_2$ for vibration-rotational spectra. In addition, it is well known that the imaginary part of $iS_1 + S_2$ is much smaller than the real part. As a result, we have neglected this imaginary part in the present study. There are no any problems to include the imaginary part in our further calculations. More explicitly, we know how to derive the matrix elements of $\text{Im}S_{2,\text{outer},i}$ and $\text{Im}S_{2,\text{outer},f}$ because we have an effective tool at handy and have had experiences to carry out these calculations.²⁹ In fact, by introducing the 2D causal correlation functions³⁰ and by carrying out the corresponding 2D Fourier transforms, one is able to obtain the 2D Hilbert transforms with which one can easily calculate these imaginary matrix elements. Meanwhile, if the potential model contains vibrational dependences, the correlation functions introduced in our formalism would depend on the vibrational quantum numbers as well. This implies that one may need to have different sets of the correlation functions in calculating the matrix elements for each of the $S_{2,\text{outer},i}$, $S_{2,\text{outer},f}$, and $S_{2,\text{middle}}$ terms. We expect that whether to distinguish these different sets is necessary or not would depend on cases of interest.

As a next research step, we will consider systems involving more complicated molecules. The target is to consider the line coupling for the H_2O-N_2 system because a lot of values of the half-width and shift of H_2O lines listed in HITRAN come from theoretically calculated results with the RB formalism. For this important system, we expect that the line coupling would happen among lines belonging to different branches and effects on calculated half-widths and shifts from the line coupling could be significant. At present, after successfully considering the line coupling for all three branches of linear molecules, we stand on a more sound position to pursue this difficult problem.

ACKNOWLEDGMENTS

We would like to thank Dr. Thibault for helpful discussions and Professor Bermejo for having provided us experimental data prior to publication. Two of the authors (Q. Ma and R. H. Tipping) acknowledge financial support from NSF under Grant No. 1228861. This research used resources of the National Energy Research Scientific Computing Center, which is supported by the Office of Science of the U.S. Department of Energy under Contract No. DE-AC02-05CH11231.

¹P. W. Anderson, *Phys. Rev.* **76**, 647 (1949).

²C. J. Tsao and B. Curmutte, *J. Quant. Spectrosc. Radiat. Transfer* **2**, 41 (1962).

³R. G. Gordon, *J. Chem. Phys.* **44**, 3083 (1966); **45**, 1649 (1966).

⁴S. Green, *J. Chem. Phys.* **62**, 2271 (1975).

⁵D. Robert and J. Bonamy, *J. Phys.* **40**, 923 (1979).

⁶C. Bloch, *Nucl. Phys.* **7**, 451 (1958).

⁷A. D. Bykov, N. N. Lavrentieva, and L. N. Sinitsa, *Atmos. Ocean. Opt.* **5**, 587 (1992); **5**, 728 (1992).

⁸J. Buldyreva, J. Bonamy, and D. Robert, *J. Quant. Spectrosc. Radiat. Transfer* **62**, 321 (1999).

⁹Q. Ma, R. H. Tipping, and C. Boulet, *J. Quant. Spectrosc. Radiat. Transfer* **103**, 588 (2007).

¹⁰Q. Ma, R. H. Tipping, and C. Boulet, *J. Chem. Phys.* **124**, 014109 (2006).

¹¹Q. Ma, C. Boulet, and R. H. Tipping, *J. Chem. Phys.* **139**, 034305 (2013). There are typos in this paper. Equation (1) should be given as $\alpha(\omega) = \frac{4\pi^2}{3\hbar c} n_a \omega (e^{\beta\hbar\omega} - 1) F(\omega)$ and Eq. (8) should be given as $\langle m(0) \rangle_{\text{bath}} = \frac{\pi}{2\pi} (1 - \hat{S})_{\text{bath}}$.

¹²M. Afzelius, P.-E. Bengtsson, and J. Bonamy, *J. Chem. Phys.* **120**, 8616 (2004).

¹³F. Thibault, L. Gómez, S. V. Ivanov, O. G. Buzykin, and C. Boulet, *J. Quant. Spectrosc. Radiat. Transfer* **113**, 1887 (2012), and references therein.

¹⁴R. Wang, *Introduction to Orthogonal Transforms with Applications in Data Processing and Analysis* (Cambridge University Press, 2012).

¹⁵F. Thibault, O. Vieuxmaire, T. Sizun, and B. Bussery-Honvault, *Mol. Phys.* **110**, 2761 (2012).

¹⁶H. Rozario, J. Garber, C. Povey, D. Hurtmans, J. Buldyreva, and A. Predoi-Cross, *Mol. Phys.* **110**, 2645 (2012).

¹⁷Q. Ma, R. H. Tipping, and R. R. Gamache, *Mol. Phys.* **108**, 2225 (2010).

¹⁸J. Boissoles, C. Boulet, D. Robert, and S. Green, *J. Chem. Phys.* **90**, 5392 (1989).

¹⁹W. B. Neilsen and R. G. Gordon, *J. Chem. Phys.* **58**, 4131 (1973).

²⁰M. R. Cherkasov, *Opt. Spectrosc.* **40**, 3 (1976); **105**, 851 (2008); **106**, 1 (2009); **107**, 553 (2009).

²¹H. J. Weaver, *Theory of Discrete and Continuous Fourier Analysis* (John Wiley and Sons, New York, 1989).

²²J. W. Cooley and J. W. Tukey, *Math. Comput.* **19**, 297–301 (1965).

²³F. Thibault, R. Z. Martinez, D. Bermejo, S. V. Ivanov, O. G. Buzykin, and Q. Ma, "An experimental and theoretical study of nitrogen broadened acetylene lines," *J. Quant. Spectrosc. Radiat. Transfer* (submitted).

²⁴M. R. Cherkasov, "Theory of relaxation parameters of the spectrum shape in the impact approximation - I: General consideration," *J. Quant. Spectrosc. Radiat. Transfer* (to be published).

²⁵V. I. Starikov, *Opt. Spectrosc.* **112**, 24–31 (2012).

²⁶V. I. Starikov, *Opt. Spectrosc.* **114**, 15–24 (2013).

²⁷J.-M. Hartmann, C. Boulet, and D. Robert, *Collisional Effects on Molecular Spectra* (Elsevier, 2008).

²⁸C. Boulet, Q. Ma, and F. Thibault, *J. Chem. Phys.* **140**, 084310 (2014).

²⁹Q. Ma, R. H. Tipping, and N. N. Lavrentieva, *J. Quant. Spectrosc. Radiat. Transfer* **113**, 936 (2012).

³⁰S. L. Hahn, *Hilbert Transform in Signal Processing* (Artech House, Boston, 1996).